Dipole and quadrupole contributions to polarized Cu *K* x-ray absorption near-edge structure spectra of CuO

S. Bocharov, Th. Kirchner, and G. Dräger
Fachbereich Physik der Martin-Luther-Universität Halle-Wittenberg, Friedemann-Bach-Platz 6, D-06108 Halle, Germany

O. Šipr and A. Šimůnek
Institute of Physics, Academy of Sciences of the Czech Republic, Cukrovarnická 10, 162 53 Praha 6, Czech Republic
(Received 5 May 2000; published 3 January 2001)

Polarized Cu *K* x-ray absorption near-edge structure spectra of CuO are measured and analyzed with the aim of extracting quadrupole and dipole partial spectral components. Theoretical spectral components are calculated within the framework of real-space multiple-scattering technique, relying on a non-self-consistent muffin-tin potential. A local coordinate system $x'y'z'$ suitable for polarization analysis is defined by the sides of the CuO_4 quasirectangle rather than by directions of the Cu-O bonds. An exclusively quadrupole nature of the prepeak is established both experimentally and theoretically. By analyzing the experimental data, we find that those states which give rise to the prepeak lie within the CuO plane, and have mainly a $d_{x'y'}$ character. The theory correctly reproduces gross features of the polarized structure generated by dipole transitions, apart from a spurious peak at 8983 eV for the $p_{z'}$ component. A partial agreement between theory and experiment in the shoulder region suggests that this structure may arise partly from one-electron states and partly from many-body processes.

DOI: 10.1103/PhysRevB.63.045104 PACS number(s): 78.70.Dm, 71.20.Nr, 74.72.−h

I. INTRODUCTION

The discovery of high-T_c superconductors invoked a renewed interest in basic physical properties of copper oxides. Among them, CuO occupies a unique position thanks to the presence of CuO_2 layers in all copper-based high-T_c materials. Low-lying unoccupied electron states of CuO were studied by means of *unpolarized*, i.e., isotropic, x-ray absorption near-edge structure (XANES) spectra extensively in the past.[1–4] However, open questions still remain—in particular, in the interpretation of the Cu *K*-edge XANES spectrum. First of all, it is not quite clear to what extent can CuO be described within a one-electron formalism, as the importance of strong electron correlations in CuO was stressed in many studies.[5–8] Second, contradictory conclusions have been reached about the nature of prominent spectral features.

For example, the distinct prepeak occurring around 10 eV below the first intensive maximum was attributed to *quadrupole* transitions on the basis of several sophisticated molecular-cluster calculations.[9–11] Another convincing evidence in favor of a significant quadrupole contribution to Cu *K*-edge prepeak in XANES of a $CuCl_4^{-2}$ complex was presented by analyzing its polarization (i.e., angular) dependence.[12] However, it is disputable to what extent the conclusions reached for a small molecular complex such as $CuCl_2$ (Ref. 9) or $CuCl_4^{2-}$ (Refs. 10 and 12) can be generalized to the case of a bulk solid CuO. A weak prepeak structure generated by *dipole* transitions alone was also obtained from one-electron real-space multiple-scattering (RS-MS) calculations for large solidlike clusters,[1,2] relying just on a non-self-consistent muffin-tin potential generated via the so-called Mattheiss prescription.[13] The energy position of the theoretical prepeak does not quite agree with experiment in those studies;[1,2] however, such a discrepancy still can be ascribed not only to the failure of a dipole approximation but alternatively also to the inadequacy of a non-self-consistent scattering potential. Note also that one-electron calculations of the electronic structure of CuO fail to reproduce, e.g., bremsstrahlung isochromat spectroscopy (BIS) spectra near the threshold as well.[6,7] Previous investigations of various bulk materials demonstrated that the prepeak can be of a purely dipole origin (as in TiS_2 and related chalcogenides[14]) or can have sizable dipole as well as quadrupole contributions—as in $VOPO_4 \cdot 2H_2O$ or V_2O_5 (cf. Refs. 15 and 16) or in $FeCO_3$ (Ref. 17). A polarization-dependence analysis like that of Hahn *et al.*[12] has not been performed for CuO yet. Similarly, no calculation of Cu *K*-edge XANES of CuO involving quadrupole transitions has been published so far.

Another controversial topic offers a shoulder half-way between the prepeak and the main peak: Molecular-oriented quantum chemistry calculations[9–11] attribute this exclusively to many-body shake-down processes, while it can be reproduced by one-electron RS-MS calculations fairly well.[1,2] A comparative analysis based on ''Natoli's rule,'' connecting peak positions with bond lengths,[18] also supports a one-electron interpretation of this shoulder.[19]

Previous analyses of Cu *K*-edge XANES of CuO were based on unpolarized spectra.[1,2,19] The same is true for the Cu L_3 edge.[6,4,8] A simultaneous analysis of Cu *K*, Cu L_3, O *K*, and BIS spectra of CuO, in terms of quasimolecular resonances,[20] dealt solely with unpolarized spectra. Only the O *K* near edge of CuO was studied by both unpolarized[6,8] and polarized[3] absorption spectroscopy. To our knowledge, no calculation of polarization-resolved densities of unoccupied states has been performed so far, although several calculations of electronic structure of CuO were published.[7,21]

On the other hand, polarized Cu *K*-edge spectra of more complex copper oxides—such as $YBa_2Cu_3O_{6+x}$ (Ref. 22), $Bi_2Sr_2CaCu_2O_{8+\delta}$ (Refs. 23 and 24) or $La_{2-x}Sr_xCuO_4$ and

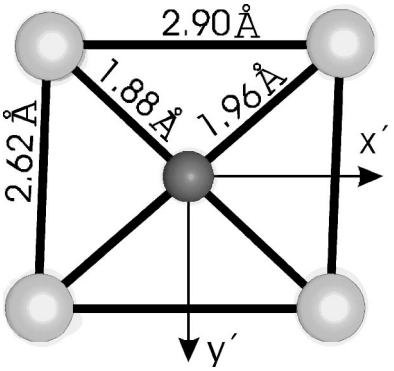

FIG. 1. Nearest coordination of a Cu atom in a CuO crystal. A planar CuO_4 complex is shown together with the orientation of the x' and y' axes relative to specific Cu-O bonds. The copper atom is in the center of the parallelogram, oxygens form its corners.

Nd_2CuO_4 (Ref. 25)—have been investigated. Similarly, studies of Cu-centered molecular complexes, on which the quadrupole interpretation of the Cu *K*-edge prepeak in CuO has relied so far, are based on polarized spectra. Hence, there is an obvious need for a polarized study of Cu *K* XANES of CuO to fill the existing gap.

It has been demonstrated that unpolarized spectra are much more tolerant to the theory than polarized spectra[16]—which, apart from offering a much more stringent test of the theory, provide an additional insight into the nature of particular spectral structures. Hence we concentrate in this study on *polarized* Cu *K*-edge spectra of CuO, and analyze them both experimentally and theoretically. Our particular aim is to determine the quadrupole or dipole nature of the prepeak.

II. CRYSTAL STRUCTURE

Cupric oxide can be considered as unique among transition-metal monoxides. While the related monoxides NiO and CoO have cubic crystal structures, CuO crystallizes in a monoclinic tetramolecular unit cell, with space group C_{2h}^6 ($2/m$, No. 15), $a=4.6837$ Å, $b=3.4226$ Å, $c=5.1288$ Å, and $\beta=99.54°$, with the Cu atom in a planar coordination of a parallelogram built of four O atoms.[26] The parallelogram contains the shortest Cu-O bonds 1.88 and 1.96 Å, and can be treated as a quasirectangle (Fig. 1). Other two much longer Cu-O bonds are not precisely perpendicular to the parallelogram plane, but rather build apexes of a strongly distorted octahedron.

The parallelograms share one vertex (i.e., one oxygen atom) with each other, forming two geometrically conjugate systems of chains running in the directions [110] and $[-110]$, and containing the shortest Cu-O bonds. The respective planes include an angle of 78°, and we denote them $x'y'$ and $x''y''$—see Fig. 2. Thus one can differentiate between two different Cu sublattices. The Cu-O bonds within each chain are coplanar and characterized through an extreme strength (as already observed at the sample preparation stage). The external face of a real CuO crystal is shaped not by the unit-cell planes, but rather by surfaces parent to Cu-O planes.

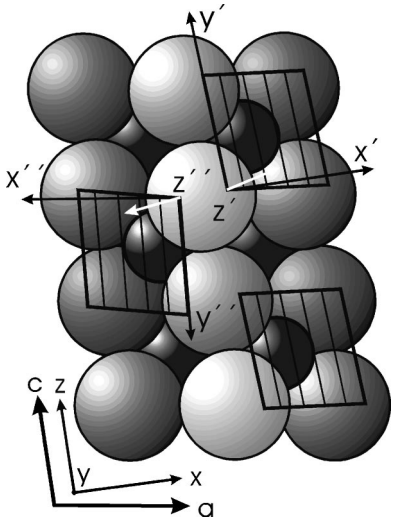

FIG. 2. CuO crystal structure projected on the ac plane. The two chain planes of types I and II are identified by the frames on the left and right halves of the diagram, respectively.

III. EXPERIMENT

A thin CuO plate of about $4\times4\times0.5$ mm^3 was cut from a crystalline sample parallel to one of the chain planes (i.e., the plane marked in Fig. 2). After a dimpling to ≈10-μm thickness, it was used as the absorption sample in a classical transmission layout. The sample orientation and crystal quality were verified using Laue patterns.

The experiments were carried out at the beam lines $A1$ and $E4$ (HASYLAB, DESY) equipped with a Si (111) two crystal monochromator. The sample plate was positioned in a PC-controlled goniometer, allowing three perpendicular rotations ϕ, θ, and ψ, so that in the beginning the direction $\boldsymbol{c}$ of the unit cell coincides with the θ axis and the polarization vector $\boldsymbol{\varepsilon}$, while the sample plate (i.e., the chain plane) is perpendicular to the beam direction (zero position with $\phi=0$, $\theta=0$, and $\psi=0$). The rotated sample position (ϕ,θ, and ψ) is expressed as $\boldsymbol{x}'=\hat{\Psi}\hat{\Theta}\hat{\Phi}\boldsymbol{x}$, while the wave vector $\boldsymbol{k}$ and polarization vector $\boldsymbol{\varepsilon}$ of the incident radiation are not effected by the rotational operators $\hat{\Psi}$, $\hat{\Theta}$, and $\hat{\Phi}$.

In order to separate the absorption resulting from *K* transitions exclusively, we used a subtraction of the background function $f(E)=a/E^4+b/E^3+c$ after Victoreen. All the spectra were corrected for an equivalent effective sample thickness, with an additional matching normalization of max$\pm5\%$ in the remote extended x-ray absorption fine structure (EXAFS) region. The normalized raw experimental spectra are displayed in Fig. 3. The quality of normalization is illustrated by appearance of a ''magic point'' at 8993 eV. The three numbers in the parentheses denote the sample positioning angles ϕ, θ, and ψ, and thus identify each spectrum. The absolute energy scale was determined by a simultaneous record of XANES of a pure Cu metal.

IV. SPECTRAL ANALYSIS

Theoretical foundations needed for extracting symmetry-resolved partial spectral components of x-ray absorption

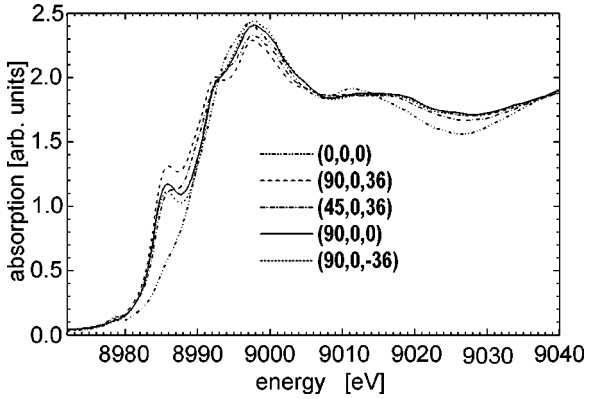

FIG. 3. Some experimental Cu *K* XANES spectra recorded at different sample orientations. Three numbers in parentheses denote the sample positioning angles ϕ, θ, and ψ for each record. Energy of the incident x rays in eV is displayed on the horizontal axis.

spectra were outlined by Brouder[27] in an extensive way. During an x-ray absorption process, the initial-state core electron, described by a wave function ψ_i, is excited into a final state described by a wave function ψ_f. This wave function can be angularly projected onto the same atom. Hence, in the region of interest, ψ_f can be written as a superposition of atomiclike wave functions with definite angular momenta:

$$\psi_f(\boldsymbol{r}) = \sum_{lm} R_l(r) Y_{lm}(\hat{\boldsymbol{r}}). \tag{1}$$

Here $R_l(r)$ and $Y_{lm}(\hat{\boldsymbol{r}})$ represent the radial and angular parts of the wave function, respectively. The dipole and quadrupole contributions to x-ray absorption cross section can be expressed via[27]

$$\mu(\hbar\omega, \boldsymbol{\varepsilon}, \boldsymbol{k}) \approx \delta(E_f - E_i - \hbar\omega)(|\langle \psi_f | \boldsymbol{\varepsilon}\cdot\boldsymbol{r} | R_0 Y_{00}\rangle|^2 + \tfrac{1}{4}|\langle \psi_f | \boldsymbol{\varepsilon}\cdot\boldsymbol{r}\,\boldsymbol{\varepsilon}\cdot\boldsymbol{k} | R_0 Y_{00}\rangle|^2) \tag{2}$$

for the *K* edge. Employing decomposition (1), Eq. (2) can be further elaborated so that one can obtain the absorption coefficient as a weighted sum of $(\boldsymbol{\varepsilon},\boldsymbol{k})$-independent partial spectral components. The weights of these components are determined by orientation of vectors $\boldsymbol{\varepsilon}$ and $\boldsymbol{k}$ with respect to the crystal.[14,27] Therefore, by recording absorption spectra for several different geometrical settings, one can use expression (2) to set up an appropriate system of linear equations, from which the partial spectral components can be extracted.

The number of individual partial spectral components crucially depends on the full point symmetry group of the crystal. For a monoclinic system, there are four independent dipole partial spectral components and nine quadrupole components.[27] This means that it is *in principle* not possible to resolve even the dipole part of the x-ray absorption spectrum into an intuitively plausible system of just three ''orthogonal'' partial components, which would reflect the projected local densities of unoccupied states (multiplied by appropriate radial matrix elements). This aspect was stressed recently by Nelhiebel *et al.*[28] who called those residuals of sum (2), which are not directly interpretable in terms of partial density-of-states (DOS) projections, ''cross-terms.''

However, the deviation of the monoclinic CuO structure from an orthorhombic one is not very large—the angle β differs from the right angle by less than 10°. For an orthorhombic structure, one would have just three partial spectral components in the dipole term. The quadrupole contribution comprises six independent components for an orthorhombic structure, and up to five components for a tetragonal system.[27] In order to simplify the analysis and to stay with physically transparent concepts as much as possible, we restrict ourselves just to *three dipole* and *five quadrupole* components in our polarization analysis, hence decomposing Eq. (2) in an approximate way as[14]

$$\mu = \mu_D + \mu_Q,$$

$$\mu_D = p_x\varepsilon_x^2 + p_y\varepsilon_y^2 + p_z\varepsilon_z^2, \tag{3}$$

$$\mu_Q = d_{xy}(\varepsilon_x k_y + \varepsilon_y k_x)^2 + d_{xz}(\varepsilon_x k_z + \varepsilon_z k_x)^2 + d_{yz}(\varepsilon_y k_z + \varepsilon_z k_y)^2 + d_{x^2-y^2}(\varepsilon_x k_x + \varepsilon_y k_y)^2 + \sqrt{3} d_{z^2}(\varepsilon_z k_z)^2, \tag{4}$$

where μ_D and μ_Q are dipole and quadrupole contributions to the absorption coefficient, respectively, and p_x, p_y, p_z, d_{xy}, d_{xz}, d_{yz}, $d_{x^2-y^2}$, and d_{z^2} denote the partial spectral components (their designation reflects the corresponding projected DOS). Note that the unpolarized quadrupole contribution (i.e., in case of a polycrystal sample) can be obtained by angular averaging of Eq. (4) as

$$\mu_Q^{(unpol)} = \frac{1}{5}d_{xy} + \frac{1}{5}d_{xz} + \frac{1}{5}d_{yz} + \frac{1}{15}d_{x^2-y^2} + \frac{1}{15}\sqrt{3}d_{z^2}. \tag{5}$$

If Eqs. (3) and (4) present a good approximation to the full equation (2), then the partial spectral components obtained by their inversion must coincide when different sets of measured polarized spectra are inserted into their left-hand sides. Hence it can be checked *a posteriori* whether the additional reduction of the number of independent partial spectral components was justified or not, and also whether the orientation of the coordinate system *xyz* was chosen in a suitable way.

V. THEORY

Polarized Cu *K*-edge XANES spectra of CuO were calculated employing the RS-MS formalism.[29] The RSMS code we used[30] is basically a modified and amended ICXANES computer code of Vvedensky, Saldin, and Pendry.[31] The calculations presented here were performed for a cluster of 95 atoms (i.e., of radius 6.0 Å), employing full multiple scattering. Coordinations of atoms[26] in finite clusters of CuO were generated with the help of the CRYSTIN crystallographic database[32] and the PICTUR code of Dušek.[33] The largest angular momentum included in the single-site scattering was $l_{max}=4$.

Non-self-consistent muffin-tin potentials were generated via the so-called Mattheiss prescription (a superposition of charge densities of isolated atoms).[13] Electron densities for

free atoms were calculated self-consistently within the local-density approximation by the LDAT code of Vackář.[34] The exchange-correlation potential of Ceperley and Adler[35] was used for atomic calculations of the occupied states. In constructing the Mattheiss potential appropriate for unoccupied states, an energy-independent $X\alpha$ potential with the Kohn-Sham value of $\alpha=0.66$ was used.[36] The muffin-tin radii of nonoverlapping spheres were determined so that single-site potentials, which were being superimposed, matched at the touching points (''matching potential condition''). The muffin-tin zero was set to the average interstitial potential. The influence of the core hole left by the excited electron was taken into account while calculating atomic charge densities by removing one electron from the core level and putting it into the lowest unoccupied atomic level (''relaxed and screened approximation'')—see, e.g., Ref. 37 for a more detailed prescription and analysis.

All theoretical results presented here include the convolution with a Lorentzian function, in order to take into account the $1s$ core hole lifetime. The full width at half-maximum (FWHM) was taken 1.5 eV according to the compilation of Al Shamma *et al.*[38]

Both dipole and quadrupole transitions were taken into account in our XANES calculation (necessary equations can be found, e.g., in the paper of Brouder[27]). As presented in Sec. IV, our partial spectral decomposition is restricted just to three *p*-like components and five *d*-like components. We identified them by means of Eqs. (3) and (4): By a suitable choice of the $\boldsymbol{\varepsilon}$ vectors and, in the case of *d*-like components, also the $\boldsymbol{k}$ vectors, all partial spectral weights vanish but one, and the partial spectral component is just equal to the calculated polarized spectrum. Only the d_{z^2} component cannot be obtained in a ''pure'' form, and was thus deduced from the quadrupole part of the $\boldsymbol{\varepsilon}=(0,1/\sqrt{2},1/\sqrt{2})$, $\boldsymbol{k}=(0,1/\sqrt{2},-1/\sqrt{2})$ spectrum, as it follows from Eq. (4) that $\mu_Q=(1/2)d_{x^2-y^2}+(\sqrt{3}/2)d_{z^2}$.

VI. RESULTS

There are two ''natural'' coordinate systems for CuO: One of them is connected with the whole unit cell, and the other is attached to the local neighborhood of the absorbing Cu atom. In the ''cell coordinate system'' xyz, the y and z axes are fixed by crystallographic axes ($y\|b,z\|c$), and x is orthogonal to them. The ''local coordinate system'' $x'y'z'$ is oriented according to the oxygen parallelogram (Fig. 1), so that the x' axis is parallel to its longer side (the O-O distance $\approx$2.9 Å), the y' axis lies within the CuO_4 parallelogram plane, and is perpendicular to x' (thereby it is nearly collinear to the shorter O-O side of $\approx$2.6 Å) and the z' axis is perpendicular to the $x'y'$ plane.

As noted in Sec. II, there are actually two interpenetrating systems of CuO_4 parallelograms in the CuO crystal (see Fig. 2). Hence when decomposing the x-ray absorption spectra in the local coordinate system, one must take into account that the raw experimental spectra reflect an *average* over two different Cu sites in two different sublattices (i.e., over coordinate systems $x'y'z'$ and $x''y''z''$ in Fig. 2). Both Cu sites are crystallographically equivalent, and hence they give rise to identical partial spectral components, except for spin-related contributions stemming from antiferromagnetic ordering of Cu atoms. However, since the spectra were recorded from a non-single-domain sample, the resolved components reproduce an average of ''spin-up'' and ''spin-down'' DOS's over all the domains. This average will be equal for both Cu sublattices, provided the resulting magnetic moments of domains are oriented randomly. Thus only the partial spectral weights vary when contributions from different Cu sites are considered.

TABLE I. Partial spectral weights evaluated from expressions (3) and (4) in both the cell and the local coordinate systems, for the same crystal orientations with respect to the $\boldsymbol{\varepsilon}$ and $\mathbf{k}$ vectors as compiled in Fig. 3. The first line corresponds to the cell coordinate system xyz, while the second line refers to the local system $x'y'z'$.

$\phi,\ \theta,\ \psi$	p_x $p_{x'}$	p_y $p_{y'}$	p_z $p_{z'}$	d_{xy} $d_{x'y'}$	d_{xz} $d_{x'z'}$	d_{yz} $d_{y'z'}$	$d_{x^2-y^2}$ $d_{x'^2-y'^2}$	d_{z^2} $d_{z'^2}$
0,0,0	0.0	0.0	1.0	0.0	0.32	0.68	0.0	0.0
	0.01	0.96	0.03	0.39	0.03	0.48	0.05	0.05
90,0,36	0.11	0.89	0.0	0.60	0.0	0.0	0.40	0.0
	0.35	0.04	0.61	0.02	0.42	0.02	0.14	0.40
45,0,36	0.0	0.65	0.35	0.34	0.27	0.0	0.22	0.17
	0.24	0.34	0.42	0.31	0.19	0.02	0.12	0.36
90,0,0	0.68	0.32	0.0	0.13	0.0	0.0	0.87	0.0
	0.56	0.01	0.42	0.02	0.73	0.03	0.07	0.15
90,0,−36	1.0	0.0	0.0	1.0	0.0	0.0	0.0	0.0
	0.68	0.0	0.32	0.03	0.13	0.01	0.21	0.62

In Table I, we summarize partial spectral weights relevant to the experimental spectra presented in Fig. 3. The weights are evaluated from Eqs. (3) and (4), for both the cell coordinate system xyz and for the local coordinate system $x'y'z'$.

A. Dipole contributions

Let us consider just the dipole terms alone. In Fig. 4 we present partial spectral components resolved from four different triads of experimental curves by inverting Eqs. (3) in the cell and in the local coordinate systems. From the good overall coincidence of the spectral components obtained from different triads, it follows that considering only three dipole components was justified, and that both xyz and $x'y'z'$ coordinate systems are suitable for the partial spectra decomposition. Note that the latter is not self-evident: We verified that an arbitrary choice of the coordinate system does not generally lead to any coincidence of solutions of systems (3). Particularly, it is interesting to note that, e.g., orienting the x' and y' axes along the shortest Cu-O bond directions does not create a good ''parental'' coordinate system (spectral densities extracted from different triads do not coincide in such a case).

B. Quadrupole contributions

Since in transition-metal compounds the empty $3d$-derived states normally lie at lower energies than the

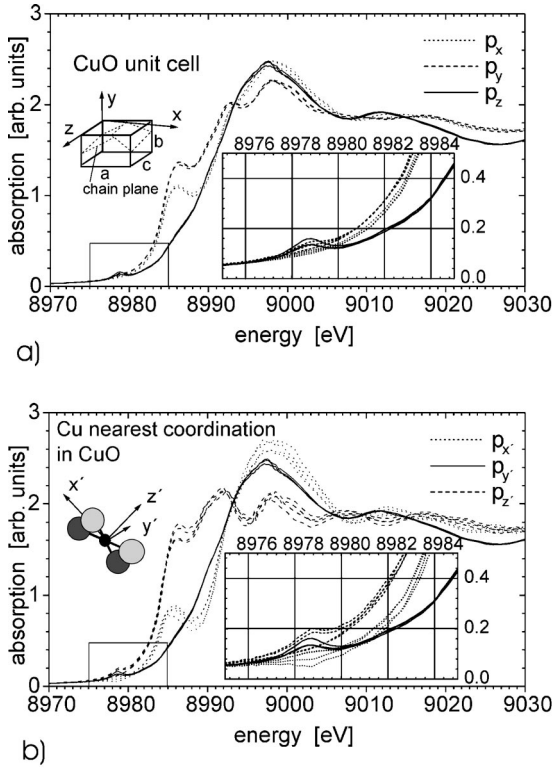

FIG. 4. Experimental Cu *K*-edge XANES resolved into partial spectral *p*-like components in the cell coordinate system (upper panel) and in the local coordinate system (lower panel). The small drawings depict the relevant coordinate systems. The horizontal axis is in eV, and the vertical scale is arbitrary. The breakdown of the dipole angular dependence is shown enlarged in the insets. The *p*-like components were resolved from four different linear systems of the form of Eq. (3).

empty $4p$-derived states, significant quadrupole transitions are most likely to occur mainly in the pre-edge region. From principal reasons, it is not possible to employ a direct inversion of the full 8×8 linear system [Eqs. (3) and (4)] as a means to extract quadrupole spectral components $d_{xy}, d_{xz}, \ldots$ from the experimental data (see the Appendix for details). Hence other procedures have to be found and applied instead. One serviceable way to identify quadrupole contributions in x-ray absorption spectra is to look for deviations from a full coincidence of partial spectral components, resolved from different sets of experimental curves, while treating all the transitions as dipole-originated.[14,16] By applying this method, it can readily be shown that the prepeak comprises at least a sizable quadrupole component: The neglect of quadrupole contributions in Sec. VI A disrupts the coincidence of curves representing partial spectral *p* components extracted from different data sets at energies around 8979 eV (see the insets in Fig. 4). We assume that the somewhat large *absolute* spread in amplitudes at higher energies (see Fig. 4, especially the right panel) is stipulated mostly by some ''technical'' factors such as background fit quality and numerical instabilities encountered when solving the system (3) (see also Ref. 16 for a corresponding analysis of V_2O_5 spectra).

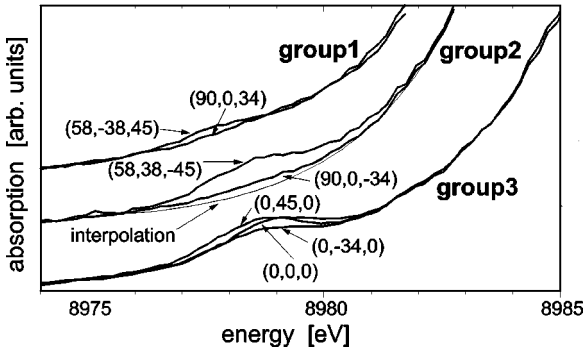

FIG. 5. Pre-edge region of Cu *K*-edge-polarized XANES. Each spectrum is identified by the sample positioning angles ϕ, θ, and ψ. The curves are associated one with another in such a way that the dipole spectral weights are identical within each group, while the quadrupole spectral weights differ. Spectral weights for each component and sample orientation are listed in Table II.

Another way to assess the extent of quadrupole contributions is to make use of experimental curves recorded at such sample-to-beam orientations that dipole spectral weights are identical, while quadrupole spectral weights differ. An illustrative set of such curves in the pre-edge region is displayed in Fig. 5. Weights of partial spectral components relevant to the respective curves are listed in Table II. The spread of individual curves belonging to identical dipole groups reflects the significance of quadrupole transitions at the prepeak.

TABLE II. Weights of spectral components of polarized Cu *K* XANES of CuO at different sample orientations (those, for which the curves displayed in Fig. 5, were recorded). Note that within each group, the dipole spectral weights are identical while the quadrupole spectral weights differ. For each particular crystal orientation (identified by positioning angles ϕ, θ, and ψ), the first line corresponds to the cell coordinate system xyz, while the second line refers to the local system $x'y'z'$.

$\phi,\ \theta,\ \psi$	p_x	p_y	p_z	d_{xy}	d_{xz}	d_{yz}	$d_{x^2-y^2}$	d_{z^2}
	$p_{x'}$	$p_{y'}$	$p_{z'}$	$d_{x'y'}$	$d_{x'z'}$	$d_{y'z'}$	$d_{x'^2-y'^2}$	$d_{z'^2}$
90,0,34	0.14	0.86	0.0	0.52	0.0	0.0	0.48	0.0
	0.35	0.04	0.61	0.02	0.44	0.02	0.14	0.38
58,−38,45	0.14	0.86	0.0	0.23	0.08	0.47	0.22	0.00
	0.35	0.04	0.61	0.15	0.25	0.34	0.18	0.08
90,0,−34	1.00	0.0	0.0	1.00	0.0	0.0	0.0	0.0
	0.68	0.0	0.32	0.03	0.12	0.02	0.21	0.62
58,38,−45	1.00	0.0	0.0	0.45	0.55	0.0	0.0	0.0
	0.68	0.0	0.32	0.37	0.06	0.18	0.10	0.29
0,45,0	0.0	0.0	1.00	0.0	0.96	0.04	0.0	0.0
	0.02	0.95	0.03	0.64	0.01	0.31	0.01	0.03
0,−34,0	0.0	0.0	1.00	0.0	0.0	1.00	0.0	0.0
	0.02	0.95	0.03	0.27	0.04	0.56	0.07	0.06
0,0,0	0.0	0.0	1.00	0.0	0.31	0.69	0.0	0.0
	0.02	0.95	0.03	0.39	0.03	0.48	0.05	0.05

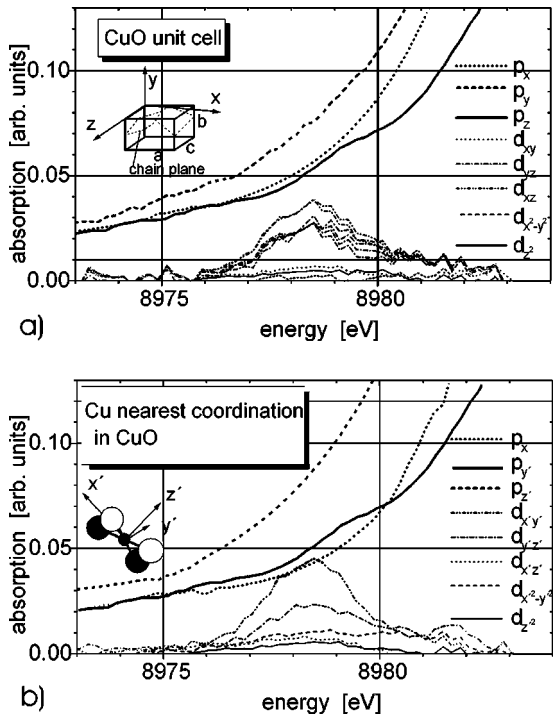

FIG. 6. Experimental Cu *K*-edge XANES in the pre-edge region, resolved into partial spectral *p*- and *d*-like components, in the cell coordinate system (upper panel) and in the local coordinate system (lower panel). The two coordinate systems, in which the partial spectral components are defined, are depicted by small drawing in each of the panel. Both dipole and quadrupole transitions are taken into account.

In order to make a more quantitative estimate of the relative ratios of the *d*-like components by inverting Eqs. (3) and (4), we need to know at least one of the partial spectral components [only then the degenerate 8×8 system of Eqs. (3) and (4) will change into a nondegenerate 7×7 system]. It can be inferred from Fig. 5 that the spectra (90,0,34) and (90,0,−34) may contain minor quadrupole contributions only. We make a ''qualified guess'' for the (90,0,−34) spectrum: A smooth curve was used to interpolate it in the pre-edge region, as shown in Fig. 5, and the small deviation of the measured (90,0,−34) spectrum from this interpolating curve was identified with the quadrupole contribution (decomposed into partial *d*-like components in the cell and the local frames according to Table II). Once one of the *d*-like components is fixed in this way, a nondegenerate (formally) 7×7 system of linear equations can be assembled from Eqs. (3) and (4), and remaining partial spectral components can be resolved. (In reality, however, we circumvented the problem of solving a potentially numerically unstable 7×7 system by uncovering the partial spectral components in a step-by-step way, employing experimental setups with special ''convenient'' values of partial spectral weights—as indicated in Table II.) The results of such a procedure are displayed in Fig. 6, both for the cell and the local coordinate systems. It is evident from Fig. 6 that the prepeak in CuO indeed is almost exclusively of a *quadrupole* nature.

To estimate the robustness of our decomposition, the d_{yz} component was extracted from four alternative linear systems and d_{xz} from two different sets in the cell coordinate system. The curves coincide rather well. Nevertheless, one should not take this coincidence too optimistically—the statistics is still not very convincing, and one must expect much worse coincidence especially at weaker intensities.

The correctness of the somewhat intuitive assumption about the nature of the (90,0,−34) spectrum made above is crucial for the *shape* of fine spectral features of the *d*-like components resolved in this way, but, at the same time, it is sufficiently robust for estimating the general ratio between partial $d_{xy}, d_{xz}, \ldots$ contributions (i.e., between areas below the peaks). In particular, we have tested that assuming the quadrupole contribution to the (90,0,-34) spectrum to be zero altogether does not lead to essential changes in the distribution of the partial spectral *d*-like components displayed in Fig. 6 (the deviations induced by these two different ''initial guesses'' fall within 10% at most).

C. Comparison between theory and experiment

Comparison between theory and experiment is displayed in Fig. 7, separately for the dipole and the quadrupole contributions. Only the local coordinate system is considered for brevity (comparing theory and experiment for the other coordinate system as well would not yield anything new). The absolute energy scale of the calculated spectrum was fixed by adjusting the energy positions of the $p_{z'}$ peak at 8998 eV. The relative positions of quadrupole and dipole theoretical components were provided by the calculation itself, however. The scaling of the vertical axis was chosen arbitrarily, so that heights of the dipole contributions would be approximately equal for the experimental and theoretical curves. The ratio between experimental and theoretical intensities of the quadrupole curves (upper frames in Fig. 7) is thus fixed, i.e., not arbitrary any more. A convolution of the theoretical spectra with a Lorentzian with a FWHM of 1.5 eV simulates the $1s$-hole lifetime broadening.

It can be seen from Fig. 7 that the theory describes well gross features of the partial *p*-like components. The ratio between $p_{x'}$, $p_{y'}$, and $p_{z'}$ intensities is generally well preserved. However, the agreement between theory and experiment is not a perfect one. The best situation is with the $p_{y'}$ component: Theory reproduces the threefold structure of the main peak (subpeaks at 8994, 8998, and 9001 eV), as well as a weak shoulder around 8986 eV. Only the very faint feature at 8990 eV does not have its counterpart in the calculated $p_{y'}$ curve. The fine structure of the main broad peak of the $p_{x'}$ component is reproduced less satisfactorily—in the theoretical spectrum, its beginning at 8995 eV is too sharp. Moreover, the distinct shoulder at 8986 eV is absent in the calculation. The worst situation emerges for the $\boldsymbol{\varepsilon}\|z'$ polarization: Theory correctly provides the peaks at ~8992 and 8998 eV, but the theoretical peak at 8986 eV has a superfluous double structure and, more seriously, there is no experimental counterpart to the peak predicted at 8983 eV.

The energy position of the quadrupole prepeak is predicted correctly by the theory, apart from a minor 1-eV shift.

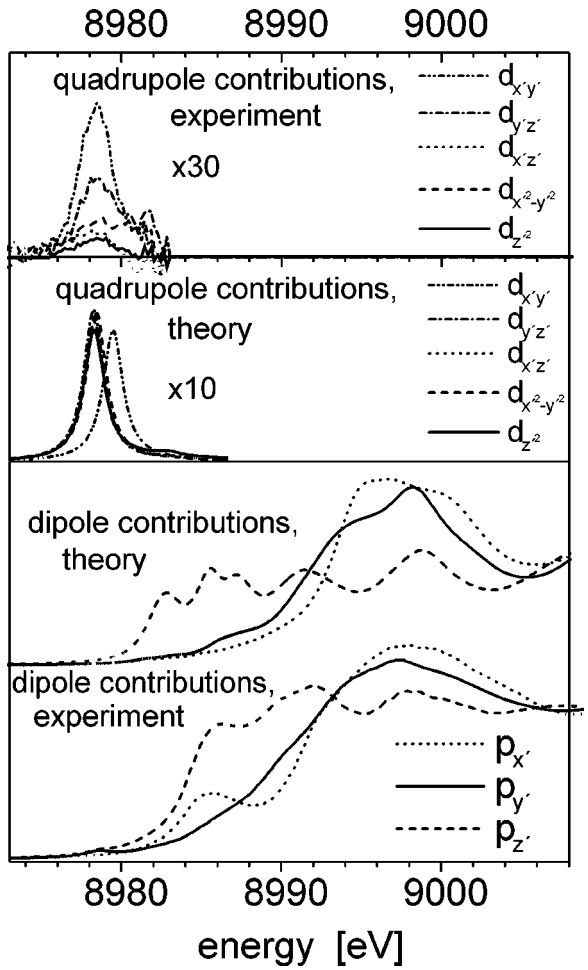

FIG. 7. Comparison of theoretical and experimental partial spectral components of Cu *K*-edge XANES in the *local* coordinate system. Dipole transitions are represented by the *p*-like components in the lower two frames, and quadrupole transitions give rise to the *d*-like components shown in the upper two frames. In the lower two frames, the dotted line denotes the $p_{x'}$ component, the solid line denotes the $p_{y'}$ component, and dashed lines denote the $p_{z'}$ component. The quadrupole-related *d*-like components in the two upper frames were multiplied by ten or 30 as indicated, in order to make them more visible.

The peak intensity of the theoretical quadrupole spectral curves is about three times higher than of the experimental ones—still, it is much lower than the intensity of dipole peaks occurring at higher energies. The overall intensity of the prepeak in the unpolarized, isotropic case, evaluated by Eq. (5) and integrated over the whole prepeak energy range (with the extent of about 8 eV), is about seven times higher for the theory than for the experiment.

Our calculation suggests that the spectral *d*-like components arise from transitions to highly localized states: The theoretical structure presented in Fig. 7 was actually generated by broadening the raw calculated spectrum, which comprises just five very intense and very narrow Lorentzian-shaped resonances. Four of them are located around 8978 eV, they are separated in energy by 0.06–0.10 eV from each other, and their FWHM's are in the range of 0.003–0.010 eV; the fifth of them is shifted by about 1 eV to higher energies, and its FWHM is about 0.02 eV. We do not display these raw theoretical curves for brevity. The predicted decomposition of the theoretical prepeak into individual *d*-like components appears to be in a disagreement with the decomposition obtained from experimental data (cf. the two upper panels of Fig. 7).

VII. DISCUSSION

The success of decomposing the experimental Cu *K*-edge XANES into just three dipole spectral components confirms our initial conjecture that deviations of CuO crystal from the orthorhombic structure are not significant in this respect. Using another terminology, the dipole cross-terms,[28] although formally present, do not give rise to observable features in this case. This is not surprising: As noted in Sec. IV, it is the deviation of the angle $\beta = 99.54°$ from the right angle, which causes the dipole-selected polarized spectra of CuO to comprise four independent components instead of merely three. As this deviation is not very large, it is natural to expect that just three components ought to be enough to describe the dipole part of the polarized Cu *K*-edge spectra of CuO.

A bit more unexpectedly, we found *from the experiment* that a consistent local coordinate system $x'y'z'$, suitable for polarized XANES analysis, has to be oriented so that the x' and y' axes are directed *parallel to the sides* of the CuO_4 parallelogram, as shown in Fig. 1. Note that in earlier publications dealing with the electronic structure of CuO (e.g., Ref. 21), local coordinate axes seem to have been oriented differently—namely, parallel to the Cu-O bonds. Nevertheless, this fact probably has only a secondary importance for physical problems. Note also that in the case of high-T_c superconductors, a suitable orientation of the x' and y' axes within the CuO_2 layers may be different than in the case of CuO, as the orthorhombic distortion of the O_4 base is much lower for high-T_c materials than for CuO.[39]

The *purely quadrupole* nature of the prepeak was established in a positive way, both experimentally and theoretically. Preliminary assignments based on investigations of $CuCl_2$ and $CuCl_4^{2-}$ molecular complexes[9–12] are thus confirmed. The reproduction of this prepeak by earlier RS-MS calculations,[1,2] which were limited to the dipole contributions only, was just a fortuitous one: The putative unpolarized ''prepeak'' actually arose from the spurious $p_{z'}$ peak at 8983 eV (see the lower two panels of Fig. 7).

We feel that only a rigorous analysis of the kind performed here, for the material in question, can be considered as sufficient to determine the quadrupole or dipole character of the prepeak. Our study thus puts on a solid ground earlier tentative attributions of quadrupole character to prepeaks in more complex copper oxides as well. In particular, e.g., Saini *et al.*[24] identified a quadrupole transition in Cu *K* XANES of $Bi_2Sr_2CaCu_2O_{8+\delta}$, relying just on a comparison of two polarized spectra. Exploiting the analogy between CuO and $Bi_2Sr_2CaCu_2O_{8+\delta}$, our study provides indirect but firm evidence in support of their conclusion.

By analyzing the experimental spectra, we found a consistent way of describing the quadrupole contribution in

terms of just five *d*-like components, which happens formally only for tetragonal and higher symmetries. However, the quadrupole prepeak is weak and in fact quite structureless, meaning that definite conclusions concerning negligibility of the *quadrupole cross-terms* cannot be drawn solely from this observation. Note that, contrary to the dipole case, the formal presence of cross-terms in the quadrupole part of Cu *K*-edge-polarized spectra of CuO is not caused just by the slight deviation of β from the right angle: Even for an orthorhombic structure, there would still be six independent components left, i.e., one too many to be interpretable in terms of *d*-like DOS-related components (cf. Sec. IV—one needs a tetragonal symmetry to reduce the number of spectral components down to five or even four). An intuitive reason why one could do with just five components only might rest in the fact that the x-ray absorption process is a local one in its nature and, hence, it is the local symmetry of the CuO_4 semirectangle which matters most. (Although, formally, it is the full point group of the crystal and not the local point group of the photoabsorber which determines the angular dependence of polarized spectra.[27]) As the deviation of the CuO_4 semirectangle from a perfect square is not a drastic one, it can be expected that no large error is generated by relying on five components only. By sticking with five *d*-like spectral components, it is also more easier to make links with previous studies, as x-ray spectra of CuO and related compounds were often treated within the tetragonal D_{4h} framework in the past.[6,20] Thus we adopt the negligibility of quadrupole cross-terms as a ''working hypothesis,'' not inconsistent with our analysis of experimental results.

As a whole, it is first of all the overall magnitude of each of the $d_{x'y'}, d_{x'z'}, \ldots$ contributions to the quadrupole prepeak (areas below the respective curves) that is provided by our analysis. The double-peak structure apparent from the uppermost panel of Fig. 7 may be an artifact. Our RS-MS calculation fails to reproduce the experiment-based decomposition of the quadrupole peak into five specific partial spectral *d*-like components. An obvious, though not very revealing, explanation at hand is the inadequacy of the scattering potential we employed for energies that close to the threshold: A non-self-consistent muffin-tin potential may be just accurate enough to reproduce the prepeak in position and intensity but insufficient to provide a correct $d_{x'y'}, d_{x'z'}, \ldots$ decomposition. This interpretation is plausible given the fact that inaccuracies in the calculation occur even at higher energies, where the details of the scattering potential ought to play an even smaller role. However, one should bear in mind that the experimental decomposition itself may also be inaccurate—due to neglect of the cross-terms (see above) and/or due to statistical errors in the experimental data. Evidently, further study seems to be necessary before the shares of individual $d_{x'y'}, d_{x'z'}, \ldots$ components in the prepeak are known more precisely and reliably. At the moment, we put more trust in the analysis of the experimental data, and assume that the prepeak is comprised mainly of the $d_{x'y'}$ component (measured in the local coordinate frame).

This finding of ours can be confronted with results of electronic structure calculations by Anisimov *et al.*[21] and Grioni *et al.*[3] Both groups discovered that the projection of the lowest unoccupied states in CuO onto the Cu site has a $d_{x^2-y^2}$ character. However, it can be deduced that their coordinate system is rotated by 45° with respect to our local coordinate frame (cf. Fig. 1), which means that their $d_{x^2-y^2}$ orbital actually corresponds to the $d_{x'y'}$ orbital in our notation. Thus it can be concluded that our experimental finding supports earlier theoretical results.[3,21] A similar conclusion in its nature—viz., that the lowest unoccupied states lie in the local $x'y'$ plane—was reached also for $Bi_2Sr_2CaCu_2O_8$ by analyzing polarization dependence of the experimental O *K* edge spectra.[40]

There is a significant disagreement between theory and experiment for the $p_{z'}$ dipole component around 8983 eV. Since our calculation relies on a non-self-consistent muffin-tin potential generated via the Mattheiss prescription, one cannot aim at a very good coincidence between experimental and theoretical curves. Nevertheless, the existence of a pronounced spurious peak in the theory is a larger failure than one would expect. This is especially surprising given the fact that our calculation correctly reproduces the position and intensity of the quadrupole peak, which is even closer to the Fermi level (and hence more prone to deficiences of the scattering potential). This reminds one of the case of the polarized V *K*-edge XANES spectra of V_2O_5, where failures of the theory for the polarized $\boldsymbol{\varepsilon} \| z$ component were also observed.[16]

It is not evident what is the cause of this failure. Tentatively we suggest, however, the breakdown of the muffin-tin approximation as the main reason: the $\boldsymbol{\varepsilon} \| x'$ and $\boldsymbol{\varepsilon} \| y'$ spectra, which mainly probe the electronic structure of more closely packed $x'y'$ planes are reproduced markedly better than the $\boldsymbol{\varepsilon} \| z'$ component, which is presumably more affected by the loose CuO structure in the z' direction. We would not disclose this failure of the theory unless polarized spectra were involved. Comparison of the theory with polarized experiments also reveals that the calculated structure provisionally identified with the prepeak in earlier theoretical studies of unpolarized spectra,[1,2] actually arose from this false $p_{z'}$ peak at 8983 eV.

The calculation describes some of the features in the shoulder structure of the polarized spectra between ~8986 and 8992 eV; however, some of the experimental peaks do not have theoretical counterparts in this energy range (especially the $p_{x'}$ peak at 8986 eV). At this energy range—around 10 eV above the edge—one can expect that the deficiencies of a non-self-consistent muffin-tin potential, employed by us, need not be very significant. Let us recall further that previous studies suggested a many-body interpretation of the shoulder structure.[9–11] Hence, in light of these facts, it seems plausible that the shoulder structure is of a *mixed origin*: In part it is of a one-electron nature, and in part it is caused by many-body shake-down processes of the kind explored by Bair and Goddard,[9] Kosugi *et al.*,[10] and Yokoyama *et al.*[11] The same argument evidently applies to the unpolarized spectra as well. Nevertheless, the purely one-electron nature of the shoulder peaks still cannot be excluded as long as a proper full-potential self-consistent study is made. On the other hand, an exclusively many-body inter-

pretation of the whole shoulder between 8986 and 8992 eV seems to be improbable in the light of our results.

The peaks of the theoretical spectrum are sharper than in the experiment, even after finite core hole lifetime smearing is applied (especially in case of $p_{x'}$ and $p_{y'}$ components). The need for additional smearing suggests a further photoelectron lifetime reduction—an effect which may have common grounds in other heavier transition metals as well.[41]

VIII. CONCLUSIONS

We found that a ''natural'' local coordinate system, suitable for analyzing low-lying unoccupied electron states, is defined by the sides of the CuO_4 quasirectangle rather than by the Cu-O bonds. The prepeak in the Cu *K*-edge XANES spectrum of CuO is a purely quadrupole one. One-electron theory, based on a non-self-consistent muffin-tin potential, correctly identifies the quadrupole prepeak and a more pronounced polarized structure generated by dipole transitions, apart from a notable failure at 8983 eV for the $p_{z'}$ component in the local frame—a breakdown which would remain uncovered if only unpolarized spectra were analyzed. By analyzing the experimental data, we find that states giving rise to the prepeak lie within the $x'y'$ plane and have mainly a $d_{x'y'}$ character, in agreement with earlier electronic structure calculations.[3,21] A partial agreement between theory and experiment in the shoulder region suggests that this structure may arise partly from one-electron states and partly from many-body processes.

ACKNOWLEDGMENTS

The experimental work was supported by Hamburger Synchrotronstrahlungslabor HA-SYLAB (Project No. II-95-67). The theoretical part was supported by project 202/99/0404 of the Grant Agency of the Czech Republic. The use of the CRYSTIN structural database was financed by grant 203/99/0067 of the Grant Agency of the Czech Republic.

APPENDIX: EXTRACTION OF QUADRUPOLE PARTIAL SPECTRAL COMPONENTS

Even if the experimental spectra were measured absolutely accurately, it still would not be possible to resolve partial spectral components of both dipole and quadrupole origin simultaneously, just by inverting the 8×8 system [Eqs. (3) and (4)]. The reason for this is that the eight spherical harmonics (or their linear combinations), on which we project the angular part of the radiatively perturbed core state, do not form an orthogonal basis. Rather, they form two orthogonal bases, namely, a three-dimensional base and a five-dimensional base—but no eight-dimensional base. Of course, the hydrogenlike wave functions (but not their angular parts) do form an orthogonal 8×8 system.

This can be observed from the fact that the partial spectral weights, which form the coefficients of the 8×8 system, conform the orthonormalization requirement for the $l=1$ and 2 cases separately:

$$\sum_{\alpha}^{x,y,z} |\langle Y_\alpha|\boldsymbol{\varepsilon}\cdot\mathbf{r}|Y_{00}\rangle|^2=1,$$

$$\sum_{\alpha}^{xy,xz,\ldots,z^2} |\langle Y_\alpha|\boldsymbol{\varepsilon}\cdot\mathbf{r}\,\boldsymbol{\varepsilon}\cdot\mathbf{k}|Y_{00}\rangle|^2=1.$$

One can check this for the particular form of spectral decomposition we use directly, by inserting the Cartesian components of the $\boldsymbol{\varepsilon}$ and $\mathbf{k}$ vectors (which can be found, e.g., in Ref. 27) into Eqs. (3) and (4), thus forming an 8×8 matrix of the coefficients. It is now straightforward to show that the determinant of this 8×8 system must be zero: If we add the second and third columns to the first, we obtain a column which has a unit value in each of its positions, similarly to what we find if we add the last four columns to the fourth one—thus obtaining two identical columns of units. Hence our 8×8 system of equations is a degenerate one, and cannot be solved unless an additional condition for the partial spectral components is employed.

[1] D. Norman, K.B. Garg, and P.J. Durham, Solid State Commun. **56**, 895 (1985).
[2] O. Šipr, J. Phys. Condens. **4**, 9389 (1992).
[3] M. Grioni, M.T. Czyżyk, F.M.F. de Groot, J.C. Fuggle, and B.E. Watts, Phys. Rev. B **39**, 4886 (1989).
[4] M. Grioni, J.B. Goedkoop, R. Schoorl, F.M.F. de Groot, J.C. Fuggle, F. Schäfers, E.E. Koch, G. Rossi, J.-M. Esteva, and R.C. Karnatak, Phys. Rev. B **39**, 1541 (1989).
[5] J. Zaanen, G.A. Sawatzky, and J.W. Allen, Phys. Rev. Lett. **55**, 418 (1985).
[6] J. Ghijsen, L.H. Tjeng, J. van Elp, H. Eskes, and M.T. Czyżyk, Phys. Rev. B **38**, 11 322 (1988).
[7] W.Y. Ching, Y.-N. Xu, and K.W. Wong, Phys. Rev. B **40**, 7684 (1989).
[8] L.H. Tjeng, C.T. Chen, and S.-W. Cheong, Phys. Rev. B **45**, 8205 (1992).
[9] R.A. Bair and W.A. Goddard III, Phys. Rev. B **22**, 2767 (1980).
[10] N. Kosugi, T. Yokoyama, K. Asakura, and H. Kuroda, Chem. Phys. **91**, 249 (1984).
[11] T. Yokoyama, N. Kosugi, and H. Kuroda, Chem. Phys. **103**, 101 (1986).
[12] J.E. Hahn, R.A. Scott, K.O. Hodgson, S. Doniach, S.R. Desjardins, and E.I. Solomon, Chem. Phys. Lett. **88**, 595 (1982).
[13] L.F. Mattheiss, Phys. Rev. **133**, A1399 (1964); **134**, A970 (1964).
[14] S. Bocharov, G. Dräger, D. Heumann, A. Šimůnek, and O. Šipr, Phys. Rev. B **58**, 7668 (1998).
[15] B. Poumellec, V. Kraizman, Y. Aifa, R. Cortes, A. Novakovich, and R. Vedrinskii, Phys. Rev. B **58**, 6133 (1998).
[16] O. Šipr, A. Šimůnek, S. Bocharov, Th. Kirchner, and G. Dräger, Phys. Rev. B **60**, 14 114 (1999).
[17] G. Dräger, R. Frahm, G. Materlik, and O. Brümmer, Phys. Status Solidi B **146**, 287 (1988).
[18] C.R. Natoli, in *EXAFS and Near Edge Structure*, edited by A. Bianconi, L. Incoccia, and S. Stipcich (Springer, Berlin, 1983), p. 43.

[19] R.N. Sinha, P. Mahto, and A.R. Chetal, Z. Phys. B: Condens. Matter **81**, 229 (1990).
[20] A.S. Vinogradov, V.N. Akimov, and A.B. Preobrazhenskii, Opt. Spektrosk. **81**, 807 (1996) [Opt. Spectrosc. **81**, 738 (1996)].
[21] V.I. Anisimov, J. Zaanen, and O.K. Andersen, Phys. Rev. B **44**, 943 (1991).
[22] J.M. Tranquada, S.M. Heald, A.R. Moodenbaugh, and Youwen Xu, Phys. Rev. B **38**, 8893 (1988).
[23] A. Bianconi, Chenxi Li, F. Campanella, S. Della Longa, I. Pettiti, M. Pompa, S. Turtù, and D. Udron, Phys. Rev. B **44**, 4560 (1991).
[24] N.L. Saini, A. Lanzara, A. Bianconi, and H. Oyanagi, Phys. Rev. B **58**, 11 768 (1998).
[25] A. Sahiner, M. Croft, S. Guha, I. Perez, Z. Zhang, M. Greenblatt, P.A. Metcalf, H. Jahns, and G. Liang, Phys. Rev. B **51**, 5879 (1995).
[26] S. Åsbrink and L.-J. Norrby, Acta Crystallogr., Sect. B: Struct. Crystallogr. Cryst. Chem. **26**, 8 (1970).
[27] C. Brouder, J. Phys.: Condens. Matter **2**, 701 (1990).
[28] M. Nelhiebel, P.-H. Louf, P. Schattschneider, P. Blaha, K. Schwarz, and B. Jouffrey, Phys. Rev. B **59**, 12 807 (1999).
[29] D.D. Vvedensky, in *Unoccupied Electron States*, edited by J.C. Fuggle and J.E. Inglesfield (Springer, Berlin, 1992), p. 139.
[30] O. Šipr, computer code RSMS, Institute of Physics AS CR, Praha, 1996–1999.
[31] D.D. Vvedensky, D.K. Saldin, and J.B. Pendry, Comput. Phys. Commun. **40**, 421 (1986).
[32] G. Bergerhoff, R. Hundt, R. Sievers, and I.D. Brown, J. Chem. Inform. Comput. Sci. **23**, 66 (1983).
[33] M. Dušek, computer code PICTUR, Institute of Physics AS CR, Praha, 1994.
[34] J. Vackář, computer code LDAT, Institute of Physics AS CR, Praha, 1986.
[35] See, e.g., W.E. Pickett, Comput. Phys. Rep. **9**, 115 (1989).
[36] W. Kohn and L.J. Sham, Phys. Rev. **140**, A1133 (1965).
[37] O. Šipr, P. Machek, A. Šimůnek, J. Vackář, and J. Horák, Phys. Rev. B **56**, 13 151 (1997).
[38] F. Al Shamma, M. Abbate, and J.C. Fuggle, in *Unoccupied Electron States*, edited by J.C. Fuggle and J.E. Inglesfield (Springer, Berlin, 1992), p. 347.
[39] S.S. Lederman and R. Barton, Phys. Rev. B **39**, 11 648 (1989); K.B. Blagoev and L.T. Wille, *ibid.* **48**, 6588 (1993); A. Sedky, A. Gupta, V.P.S. Awana, and A.V. Narlikar, *ibid.* **58**, 12 495 (1998).
[40] P. Kuiper, M. Grioni, G.A. Sawatzky, D.B. Mitzi, A. Kapitulnik, A. Santaniello, P. de Padova, and P. Thiry, Physica C **157**, 260 (1989).
[41] R.V. Vedrinskii (unpublished).